

## SOLITARY WAVE EFFECTS OF WOODS–SAXON POTENTIAL IN SCHRÖDINGER EQUATION WITH 3D CUBIC NONLINEARITY

*Mustafa Inc<sup>1</sup>, Muhammad Sajid Iqbal <sup>2,3</sup>, Ali Hasan Ali <sup>4,5,6</sup>,*  
*Zuha Manzoor <sup>7</sup>, Farrah Ashraf <sup>7</sup>*

<sup>1</sup>Firat University, Elazig, Turkey

<sup>2</sup>Oryx Universal College with Liverpool John Moores University, Doha, Qatar

<sup>3</sup>National University of Sciences and Technology, Islamabad, Pakistan

<sup>4</sup>University of Basrah, Basrah, Iraq

<sup>5</sup>Al-imam University College, Balad, Iraq

<sup>6</sup>Al-Ayen University, Dhi Qar, Iraq

<sup>7</sup>University of Lahore, Punjab, Pakistan

E-mail: minc@firat.edu.tr, sajid606@gmail.com, ali.hasan@science.unideb.hu,  
 zuha.manzoor10@gmail.com, farrah.ashraf@math.uol.edu.pk

In this research article, we apply the generalized projective Riccati equation method to construct traveling wave solutions of the 3d cubic focusing nonlinear Schrödinger equation with Woods–Saxon potential. The generalized projective Riccati equation method is a powerful and effective mathematical tool for obtaining exact solutions of nonlinear partial differential equations, and it allows us to derive a variety of traveling wave solutions of the 3d cubic focusing nonlinear Schrödinger equation with Woods–Saxon potential. These solutions contain periodic wave solutions, bright and dark soliton solutions. The study of many physical systems, such as Bose–Einstein condensates and nonlinear optics, that give rise to the nonlinear Schrödinger equation. We provide a detailed description of the generalized projective Riccati equation method in the paper, and demonstrate its usefulness in solving the nonlinear Schrödinger equation with Woods–Saxon potential. We present various graphical representations of the obtained solutions using MATLAB software, and analyze their characteristics. Our results provide new insights into the behavior of the 3d cubic focusing nonlinear Schrödinger equation with Woods–Saxon potential, and have potential applications in numerous fields of physics, as well as nonlinear optics and condensed matter physics.

*Keywords:* 3d cubic focusing nonlinear Schrödinger equation; Woods–Saxon potential; traveling wave solution; generalized projective Riccati equation method (GPREM).

## Introduction

The development of the wave function of a quantum particle in a nonlinear system is represented by the nonlinear Schrödinger equation which is a partial differential equation. Important applications of the nonlinear Schrödinger equation with a potential term are observed in many branches of physics, including as condensed matter physics, nonlinear optics, and plasma physics. It is specifically used to explain the dynamics of Bose–Einstein condensates, which are extremely cold atom gas combinations that can display remarkable nonlinear behaviours. The relationship between the particle and its surrounding environment is described by the potential term in the nonlinear Schrödinger equation. The physical system under examination will determine which potential to use. For instance, harmonic potentials are frequently utilized in solid-state physics, while Coulomb potentials

are frequently used in the study of atomic and molecular systems. In quantum mechanics, there are various types of potentials, including: Eckart potential [1–3], improved Rosen–Morse potential [4–6], Pöschl–Teller potential [7, 8], Coulomb potential [9], Hulthen potential [10], degenerate potential [11, 12], competing potential functions [13] and  $\mathcal{PT}$ -symmetric potentials [14–18]. Several other related studies can be seen in [19, 20].

A partial differential equation that describes the behaviour of wave packets in nonlinear media with a spatially changing refractive index is the 3d cubic focusing nonlinear Schrödinger equation with Woods–Saxon potential. It is a particular form of the nonlinear Schrödinger equation, which is a fundamental equation in many other physics domains, including nonlinear optics. The Woods–Saxon potential is a core potential with a “diffuse” tail region at very large distances and a “pocket” space in the center. It is frequently used to represent the movement of waves in nonlinear media and to describe the movement of particles in atomic nuclei. The Woods–Saxon potential affects the dispersion relation of the waves in the structure of the 3d cubic focusing nonlinear Schrödinger equation, main effects including wave guiding, self-focusing, and beam shaping.

We can write the equation as follows:

$$i\phi_t + \Delta\phi - P(x, y, z)\phi + |\phi|^2\phi = 0,$$

where  $\phi(x, y, z, t)$  is the complex-valued wave function, and  $P(x, y, z)$  is the Woods–Saxon potential with the following form [21]

$$P(x, y, z) = \frac{P_0}{1 + e^{\alpha(x+y+z)}},$$

where  $P_0$  and  $\alpha$  are arbitrary constants that define the shape and strength of the potential.

The generalized projective Riccati equation method (GPREM) [22, 23] is a mathematical method used for determining exact solutions of nonlinear ordinary differential equations. It is a development of the traditional Riccati equation method, a widely used technique for evaluating nonlinear ordinary differential equations. The generalized projective Riccati equation method involves converting a given nonlinear ordinary differential equation into a particular type of second-order ordinary differential equation known as the generalized Riccati equation. Numerous nonlinear ordinary differential equations have been successfully solved using the generalized projective Riccati equation method in a wide range of science and engineering disciplines, including control theory, fluid dynamics, mathematical physics, and mathematical biology. For problems involving dynamical systems with singularities or boundary conditions, it has been found to be particularly beneficial.

The article is organized as follows: Section 1, describes algorithm of the generalized projective Riccati equation method. Section 2 provides the application of generalized projective Riccati equation method to the 3d cubic focusing nonlinear Schrödinger equation. Section 3 gives various kinds of graphical representation to aid visualize the results of the study. The physical interpretation of the results and the conclusion are presented in Section 4, which highlights the major conclusions, points out the study’s merits and demerits, and suggests potential areas for future research.

## 1. Algorithm of Generalized Projective Riccati Equation Method

In this section, we discuss the methodology of generalized projective Riccati equation method. Consider the nonlinear partial differential equations (NLPDEs) of the following form:

$$Q(\phi, \phi_t, \phi_x, \phi_{ty}, \phi_{txz}, \dots) = 0, \quad (1)$$

where  $\phi(x, y, z, t)$  is a unknown function,  $Q$  is a polynomial in  $\phi = \phi(x, y, z, t)$ . The following are the basic steps of the generalized projective Riccati equation method:

**Step 1.** Consider a traveling wave solution with the transformation shown below:

$$\phi = \Phi(\zeta), \quad \zeta = x + y + z - vt, \quad (2)$$

where  $v$  is wave speed.

**Step 2.** Substituting Eq. (2) into Eq. (1), we obtain the following nonlinear ordinary differential equation (NLODE)

$$Q(\Phi, \Phi', \Phi'', \Phi''', \dots) = 0. \quad (3)$$

**Step 3.** Calculating the positive integer  $N$  by balancing the nonlinear term and highest order derivatives in Eq. (3).

**Step 4.** The formal solutions of Eq. (3) are given below:

**Type 1:** If  $G \neq 0$ , then

$$\Phi(\zeta) = A_0 + \sum_{i=1}^N \lambda^{i-1}(\zeta)[A_i \lambda(\zeta) + B_i \mu(\zeta)], \quad (4)$$

where the constant coefficients  $A_i, B_i (0 \leq i \leq N)$ . The functions  $\lambda(\zeta)$  and  $\mu(\zeta)$  satisfy the ordinary differential equations.

$$\begin{aligned} \lambda'(\zeta) &= \epsilon \lambda(\zeta) \mu(\zeta), \\ \mu'(\zeta) &= G + \epsilon \mu^2(\zeta) - \tau \lambda(\zeta), \quad \epsilon = \pm 1, \end{aligned} \quad (5)$$

such that

$$\mu^2(\zeta) = -\epsilon \left[ G - 2\tau \lambda(\zeta) + \frac{\tau^2 - 1}{G} \lambda^2(\zeta) \right], \quad (6)$$

where  $G$  and  $\tau$  are arbitrary constants.

**Type 2:** If  $G = \tau = 0$ , then

$$\Phi(\zeta) = \sum_{i=0}^N A_i \mu^i(\zeta), \quad (7)$$

where  $\mu(\zeta)$  satisfies the ODE

$$\mu'(\zeta) = \mu^2(\zeta). \quad (8)$$

**Step 5.**

(1) when  $G \neq 0$ , substituting Eq. (4) into Eq. (3);

(2) when  $G = \tau = 0$ , substituting Eq. (7) into Eq. (3);

obtain set of system of equations for  $\lambda^j \mu^i$ ,  $j = 0, 1, 2, \dots$ ,  $i = 0, 1$ . The coefficients of  $\lambda^j \mu^i$  terms, can be set to zero and yield a determined collection of system of equations in the variables  $\tau, A_i, B_i$  and  $G$ .

**Step 6.** The values of  $A_i, B_i$  and  $G$  are obtained by using Maple to solve system of algebraic equations.

**Step 7.** We know the existence of the following solutions that Eq. (5) uses:

Familay 1: If  $\epsilon = -1, G \neq 0$ ,

$$\lambda_1 = \frac{G \operatorname{sech}(\sqrt{G}\zeta)}{\tau \operatorname{sech}(\sqrt{G}\zeta) + 1}, \quad \mu_1 = \frac{\sqrt{G} \tanh(\sqrt{G}\zeta)}{\tau \operatorname{sech}(\sqrt{G}\zeta) + 1}, \quad (9)$$

$$\lambda_2 = \frac{G \operatorname{csch}(\sqrt{G}\zeta)}{\tau \operatorname{csch}(\sqrt{G}\zeta) + 1}, \quad \mu_1 = \frac{\sqrt{G} \coth(\sqrt{G}\zeta)}{\tau \operatorname{csch}(\sqrt{G}\zeta) + 1}. \quad (10)$$

Familay 2: If  $\epsilon = 1, G \neq 0$ ,

$$\lambda_3 = \frac{G \sec(\sqrt{G}\zeta)}{\tau \sec(\sqrt{G}\zeta) + 1}, \quad \mu_3 = \frac{\sqrt{G} \tan(\sqrt{G}\zeta)}{\tau \sec(\sqrt{G}\zeta) + 1}, \quad (11)$$

$$\lambda_4 = \frac{G \csc(\sqrt{G}\zeta)}{\tau \csc(\sqrt{G}\zeta) + 1}, \quad \mu_1 = \frac{\sqrt{G} \cot(\sqrt{G}\zeta)}{\tau \csc(\sqrt{G}\zeta) + 1}. \quad (12)$$

Familay 3: If  $G = \tau = 0$ ,

$$\lambda_5 = \frac{Q}{\zeta}, \quad \mu_3 = \frac{1}{\epsilon \zeta}, \quad (13)$$

where  $Q$  is a real constant.

## 2. Application of Generalized Projective Riccati Equation Method

Consider  $(1+1)$  dimensional 3d cubic focusing nonlinear Schrödinger equation:

$$i \phi_t = \Delta \phi - P(x, y, z) \phi + |\phi|^2 \phi = 0, \quad (14)$$

where  $\phi(x, y, z, t)$  is a complex wave function. Consider the following wave transformation for traveling wave solutions

$$\phi(x, y, z, t) = \Phi(\zeta) e^{i\delta}, \quad \zeta = x + y + z - c(x, y, z)t, \quad \delta = -\kappa x + \omega t + \theta, \quad (15)$$

where  $\Phi(\zeta)$  is the amplitude component and  $e^{i\delta}$  is the phase component of the solitary wave solution, and  $x, y$  and  $z$  is the spatial variables,  $t$  is the temporal variable,  $c(x, y, z)$  is real function. Furthermore  $\kappa$ ,  $\omega$ , and  $\theta$  represent soliton frequency, wave number, and phase constant respectively.

Substituting Eq. (15) into Eq. (14), the following constraint condition [24] for the imaginary part is given by:

$$c(x, y, z) = -6\kappa, \quad (16)$$

and for the real part, we have:

$$-3, \Phi''(\zeta) + (\omega + 3\kappa^2 + P(x, y, z)), \Phi(\zeta) - \Phi^3(\zeta) = 0. \quad (17)$$

Balancing the highest order derivative  $\Phi''(\zeta)$  along with nonlinear term  $\Phi^3(\zeta)$  in Eq. (16), we obtain  $N = 1$ . Hence formal solution of Eq. (16) is

$$\Phi(\zeta) = A_0(x, y, z) + A_1(x, y, z) \lambda(\zeta) + B_1(x, y, z) \mu(\zeta), \quad (18)$$

where  $A_0(x, y, z)$ ,  $A_1(x, y, z)$  and  $B_1(x, y, z)$  are functions and  $\lambda(\zeta)$  and  $\mu(\zeta)$  satisfies the ODE of Eq. (5) and (6).

Eq. (18) through 5 and 6 are substituted into Eq. (17) using Maple to produce a set of mathematical equations for  $\lambda^j(\zeta) \mu^i(\zeta)$  ( $j = 0, 1, \dots, i = 0, 1$ ). The coefficients of  $\lambda^j \mu^i$  terms, can be set to zero and yield a determined collection of mathematical equations in the variables  $A_0(x, y, z)$ ,  $A_1(x, y, z)$ ,  $B_1(x, y, z)$ , and  $G$ .

$$\left\{ \begin{array}{l} -3GA_1^2(x, y, z)B_1(x, y, z) + 6\epsilon^3\tau^2B_1(x, y, z) - \epsilon B_1^3(x, y, z) - \\ -6\epsilon^3B_1(x, y, z) + \epsilon\tau^2B_1^3(x, y, z) = 0, \\ 3\epsilon\tau GB_1(x, y, z) - 6GA_0(x, y, z)A_1(x, y, z)B_1(x, y, z) - \\ -2\epsilon\tau GB_1^3(x, y, z) - 6\epsilon^3\tau GB_1(x, y, z) = 0, \\ \kappa^2GB_1(x, y, z) + GP(x, y, z)B_1(x, y, z) + \epsilon G^2B_1^3(x, y, z) + \\ +G\omega B_1(x, y, z) - 3GA_0^2(x, y, z)B_1(x, y, z) = 0, \\ -GA_1^3(x, y, z) - 3\epsilon A_1(x, y, z)B_1^2(x, y, z) + 6\epsilon^3\tau^2A_1(x, y, z) - \\ -6\epsilon^3A_1(x, y, z) + 3\epsilon\tau^2A_1(x, y, z)B_1^2(x, y, z) = 0, \\ 3\epsilon\tau^2A_0(x, y, z)B_1^2(x, y, z) + 3\epsilon\tau GA_1(x, y, z) - \\ -6\epsilon\tau GA_1(x, y, z)B_1^2(x, y, z) - 3\epsilon A_0(x, y, z)B_1^2(x, y, z) - \\ -12\epsilon^3\tau GA_1(x, y, z) - 3GA_0(x, y, z)A_1^2(x, y, z) = 0, \\ -6\epsilon\tau GA_0(x, y, z)B_1^2(x, y, z) - 3\epsilon G^2A_1(x, y, z) + \omega GA_1(x, y, z) + \\ +GP(x, y, z)A_1(x, y, z) + 6\epsilon^3G^2A_1(x, y, z) + \\ +3\epsilon G^2A_1(x, y, z)B_1^2(x, y, z) - 3GA_0^2(x, y, z)A_1(x, y, z) + 3\kappa^2GA_1(x, y, z) = 0, \\ \omega GA_0(x, y, z) + 3\kappa^2GA_0(x, y, z) + 3\epsilon G^2A_0(x, y, z)B_1^2(x, y, z) - \\ -GA_0^3(x, y, z) + GP(x, y, z)A_0(x, y, z) = 0. \end{array} \right. \quad (19)$$

The following solutions of the system are obtained with the help of Maple software

### Case 1

$$\left\{ \begin{array}{l} A_0(x, y, z) = \pm \frac{1}{2} \sqrt{\omega + P(x, y, z)}, A_1(x, y, z) = \pm \frac{\omega + 4\kappa^2 + P(x, y, z) + 2\epsilon G(1-2\epsilon^2)}{6G\sqrt{\omega + P(x, y, z)}}, \\ B_1(x, y, z) = \pm \frac{1}{2} \sqrt{\frac{-(\omega + 4\kappa^2 + P(x, y, z))}{\epsilon G}}, \tau = 1, G = G. \end{array} \right. \quad (20)$$

### Case 2

$$\left\{ \begin{array}{l} A_0(x, y, z) = 0, \\ A_1(x, y, z) = \pm \sqrt{\frac{6\epsilon^4(1-\tau^2)(-1+2\epsilon^2)}{P(x, y, z) + \omega + 3\kappa^2}}, B_1(x, y, z) = 0, \\ G = -\frac{1}{3} \frac{P(x, y, z) + \omega + 3\kappa^2}{\epsilon(-1+2\epsilon^2)}. \end{array} \right. \quad (21)$$

### Case 3

$$\left\{ \begin{array}{l} A_0(x, y, z) = \pm \frac{1}{2} \sqrt{\omega + P(x, y, z)}, A_1(x, y, z) = 0, \\ B_1(x, y, z) = \pm \frac{1}{2} \sqrt{-\frac{\omega + P(x, y, z) + 4\kappa^2}{\epsilon G}}. \end{array} \right. \quad (22)$$

Plugging 20, 21, and 22 along with Eq. (18) into Eq. (17) and then Eq. (15) for solitary wave solutions:

**Case 1:** If  $\epsilon = -1, G \neq 0$ ,

$$\begin{aligned} \phi_{1,1}(x, y, z, t) &= \\ &= \left[ \pm \frac{1}{2} \sqrt{\omega + P(x, y, z)} \pm \frac{\omega + 4\kappa^2 + P(x, y, z) + 2\epsilon G(1-2\epsilon^2)}{6G\sqrt{\omega+P(x,y,z)}} \times \right. \\ &\times \left. \left( \frac{G \operatorname{sech}(\sqrt{G}\zeta)}{\tau \operatorname{sech}(\sqrt{G}\zeta) + 1} \right) \pm \frac{1}{2} \sqrt{\frac{-(\omega + 4\kappa^2 + P(x, y, z))}{\epsilon G}} \left( \frac{\sqrt{G} \tanh(\sqrt{G}\zeta)}{\tau \operatorname{sech}(\sqrt{G}\zeta) + 1} \right) \right] e^{i\delta}, \end{aligned} \quad (23)$$

$$\begin{aligned} \phi_{1,2}(x, y, z, t) &= \\ &= \left[ \pm \frac{1}{2} \sqrt{\omega + P(x, y, z)} \pm \frac{\omega + 4\kappa^2 + P(x, y, z) + 2\epsilon G(1-2\epsilon^2)}{6G\sqrt{\omega+P(x,y,z)}} \times \right. \\ &\times \left. \left( \frac{G \operatorname{csch}(\sqrt{G}\zeta)}{\tau \operatorname{csch}(\sqrt{G}\zeta) + 1} \right) \pm \frac{1}{2} \sqrt{\frac{-(\omega + 4\kappa^2 + P(x, y, z))}{\epsilon G}} \left( \frac{\sqrt{G} \coth(\sqrt{G}\zeta)}{\tau \operatorname{csch}(\sqrt{G}\zeta) + 1} \right) \right] e^{i\delta}, \end{aligned} \quad (24)$$

where  $\zeta = x + y + z - c(x, y, z)t$  and  $\delta = -\kappa x + \omega t + \theta$ .

If  $\epsilon = 1, G \neq 0$ ,

$$\begin{aligned} \phi_{1,3}(x, y, z, t) &= \\ &= \left[ \pm \frac{1}{2} \sqrt{\omega + P(x, y, z)} \pm \frac{\omega + 4\kappa^2 + P(x, y, z) + 2\epsilon G(1-2\epsilon^2)}{6G\sqrt{\omega+P(x,y,z)}} \times \right. \\ &\times \left. \left( \frac{G \sec(\sqrt{G}\zeta)}{\tau \sec(\sqrt{G}\zeta) + 1} \right) \pm \frac{1}{2} \sqrt{\frac{-(\omega + 4\kappa^2 + P(x, y, z))}{\epsilon G}} \left( \frac{\sqrt{G} \tan(\sqrt{G}\zeta)}{\tau \sec(\sqrt{G}\zeta) + 1} \right) \right] e^{i\delta}, \end{aligned} \quad (25)$$

$$\begin{aligned} \phi_{1,4}(x, y, z, t) &= \\ &= \left[ \pm \frac{1}{2} \sqrt{\omega + P(x, y, z)} \pm \frac{\omega + 4\kappa^2 + P(x, y, z) + 2\epsilon G(1-2\epsilon^2)}{6G\sqrt{\omega+P(x,y,z)}} \times \right. \\ &\times \left. \left( \frac{G \csc(\sqrt{G}\zeta)}{\tau \csc(\sqrt{G}\zeta) + 1} \right) \pm \frac{1}{2} \sqrt{\frac{-(\omega + 4\kappa^2 + P(x, y, z))}{\epsilon G}} \left( \frac{\sqrt{G} \cot(\sqrt{G}\zeta)}{\tau \csc(\sqrt{G}\zeta) + 1} \right) \right] e^{i\delta}, \end{aligned}$$

where  $\zeta = x + y + z - c(x, y, z)t$  and  $\delta = -\kappa x + \omega t + \theta$ .

**Case 2:** If  $\epsilon = -1, G \neq 0$ ,

$$\phi_{2,1}(x, y, z, t) = \left[ \pm \sqrt{\frac{6\epsilon^4(1-\tau^2)(-1+2\epsilon^2)}{P(x, y, z) + \omega + 3\kappa^2}} \left( \frac{G \operatorname{sech}(\sqrt{G}\zeta)}{\tau \operatorname{sech}(\sqrt{G}\zeta) + 1} \right) \right] e^{i\delta}, \quad (26)$$

$$\phi_{2,2}(x, y, z, t) = \left[ \pm \sqrt{\frac{6\epsilon^4(1-\tau^2)(-1+2\epsilon^2)}{P(x, y, z) + \omega + 3\kappa^2}} \left( \frac{G \operatorname{csch}(\sqrt{G}\zeta)}{\tau \operatorname{csch}(\sqrt{G}\zeta) + 1} \right) \right] e^{i\delta}, \quad (27)$$

where  $\zeta = x + y + z - c(x, y, z)t$ ,  $\delta = -\kappa x + \omega t + \theta$  and  $G = -\frac{1}{3} \frac{P(x, y, z) + \omega + 3\kappa^2}{\epsilon(-1+2\epsilon^2)}$ .

If  $\epsilon = 1, G \neq 0$ ,

$$\phi_{2,3}(x, y, z, t) = \left[ \pm \sqrt{\frac{6\epsilon^4(1-\tau^2)(-1+2\epsilon^2)}{P(x, y, z) + \omega + 3\kappa^2}} \left( \frac{G \sec(\sqrt{G}\zeta)}{\tau \sec(\sqrt{G}\zeta) + 1} \right) \right] e^{i\delta}, \quad (28)$$

$$\phi_{2,4}(x, y, z, t) = \left[ \pm \sqrt{\frac{6\epsilon^4(1-\tau^2)(-1+2\epsilon^2)}{P(x, y, z) + \omega + 3\kappa^2}} \left( \frac{G \csc(\sqrt{G}\zeta)}{\tau \csc(\sqrt{G}\zeta) + 1} \right) \right] e^{i\delta}, \quad (29)$$

where  $\zeta = x + y + z - c(x, y, z)t$ ,  $\delta = -\kappa x + \omega t + \theta$  and  $G = -\frac{1}{3} \frac{P(x, y, z) + \omega + 3\kappa^2}{\epsilon(-1+2\epsilon^2)}$ .

**Case 3:** If  $\epsilon = -1, G \neq 0$ ,

$$\begin{aligned} & \phi_{3,1}(x, y, z, t) = \\ &= \left[ \pm \frac{1}{2} \sqrt{\omega + P(x, y, z)} \pm \frac{1}{2} \sqrt{-\frac{\omega + P(x, y, z) + 4\kappa^2}{\epsilon G}} \left( \frac{\sqrt{G} \tanh(\sqrt{G}\zeta)}{\tau \operatorname{sech}(\sqrt{G}\zeta) + 1} \right) \right] e^{i\delta}, \end{aligned} \quad (30)$$

$$\begin{aligned} & \phi_{3,2}(x, y, z, t) = \\ &= \left[ \pm \frac{1}{2} \sqrt{\omega + P(x, y, z)} \pm \frac{1}{2} \sqrt{-\frac{\omega + P(x, y, z) + 4\kappa^2}{\epsilon G}} \left( \frac{\sqrt{G} \coth(\sqrt{G}\zeta)}{\tau \operatorname{csch}(\sqrt{G}\zeta) + 1} \right) \right] e^{i\delta}, \end{aligned} \quad (31)$$

where  $\zeta = x + y + z - c(x, y, z)t$  and  $\delta = -\kappa x + \omega t + \theta$ .

If  $\epsilon = 1, G \neq 0$ ,

$$\begin{aligned} & \phi_{3,3}(x, y, z, t) = \\ &= \left[ \pm \frac{1}{2} \sqrt{\omega + P(x, y, z)} \pm \frac{1}{2} \sqrt{-\frac{\omega + P(x, y, z) + 4\kappa^2}{\epsilon G}} \left( \frac{\sqrt{G} \tan(\sqrt{G}\zeta)}{\tau \sec(\sqrt{G}\zeta) + 1} \right) \right] e^{i\delta}, \end{aligned} \quad (32)$$

$$\begin{aligned} & \phi_{3,4}(x, y, z, t) = \\ &= \left[ \pm \frac{1}{2} \sqrt{\omega + P(x, y, z)} \pm \frac{1}{2} \sqrt{-\frac{\omega + P(x, y, z) + 4\kappa^2}{\epsilon G}} \left( \frac{\sqrt{G} \cot(\sqrt{G}\zeta)}{\tau \csc(\sqrt{G}\zeta) + 1} \right) \right] e^{i\delta}, \end{aligned} \quad (33)$$

where  $\zeta = x + y + z - c(x, y, z)t$  and  $\delta = -\kappa x + \omega t + \theta$ .

### 3. The Graphical Representation

In this Section, we presented 3D and contour representations that demonstrate the effects of Woods–Saxon potential on the solutions of 3d cubic focusing nonlinear Schrödinger equation.

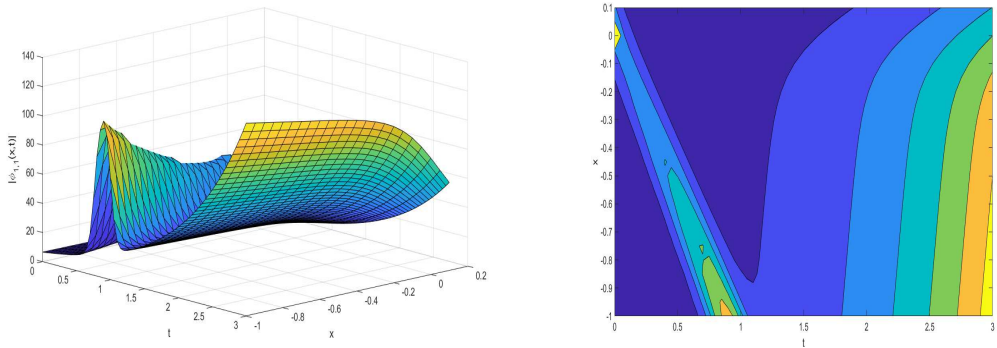


**Fig. 1.** 3-D and contour graphs of 23 for values of  $G = 500$ ,  $\tau = 10$ ,  $\alpha = 10$ ,  $P_0 = 15$ ,  $\kappa = 0, 19$ ,  $\omega = 1$ ,  $\theta = 1$

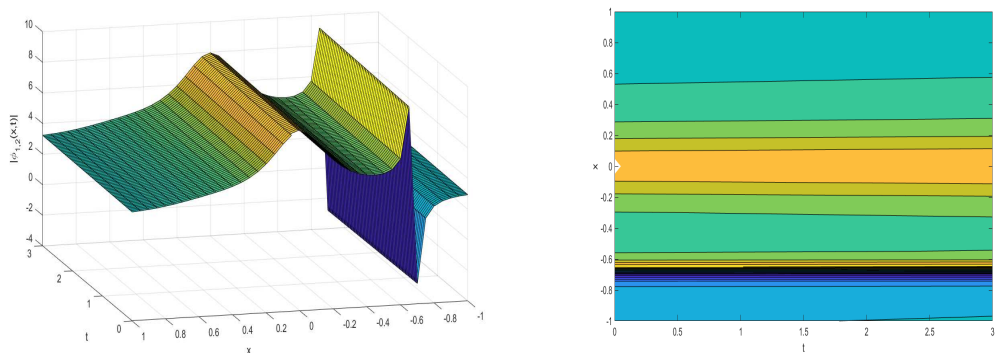


**Fig. 2.** 3-D and contour graphs of 24 for values of  $G = 50$ ,  $\tau = 60$ ,  $\alpha = 0, 1$ ,  $P_0 = 10$ ,  $\kappa = 0, 00001$ ,  $\omega = 0, 01$ ,  $\theta = 1$

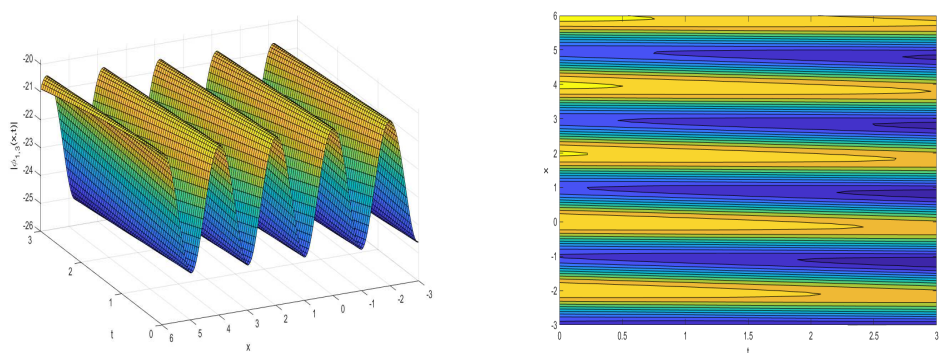


**Fig. 3.** 3-D and contour graphs of 25 for values of  $G = 10$ ,  $\tau = 10$ ,  $\alpha = 0, 1$ ,  $P_0 = 0, 01$ ,  $\kappa = 0, 01$ ,  $\omega = 0, 01$ ,  $\theta = 1$

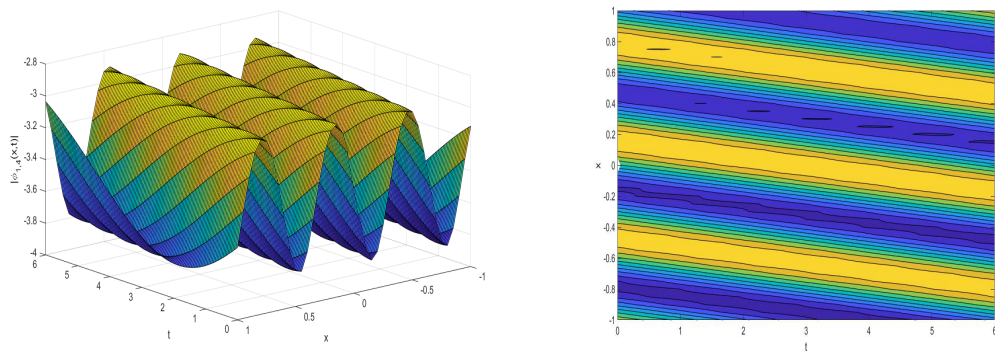


**Fig. 4.** 3-D and contour graphs of 26 for values of  $G = 100$ ,  $\tau = 10$ ,  $\alpha = 0,001$ ,  $P_0 = 10$ ,  $\kappa = 0,009$ ,  $\omega = 0,0001$ ,  $\theta = 0,001$

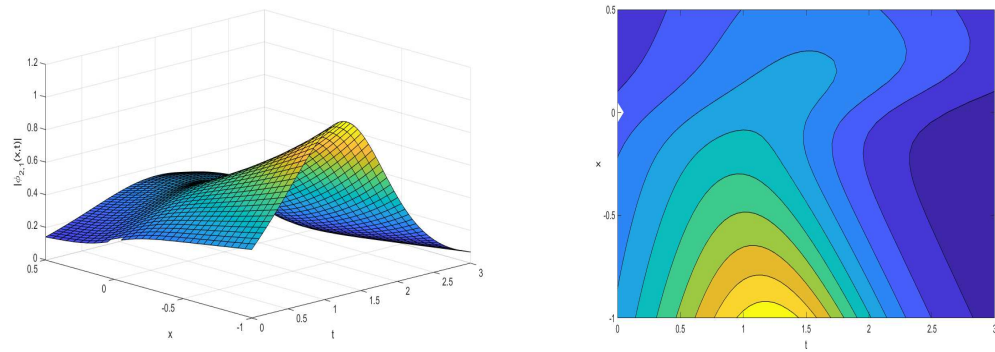


**Fig. 5.** 3-D and contour graphs of 26 for values of  $\tau = 15$ ,  $\alpha = 10$ ,  $P_0 = 2,5$ ,  $\kappa = 0,45$ ,  $\omega = 1$ ,  $\theta = 1$

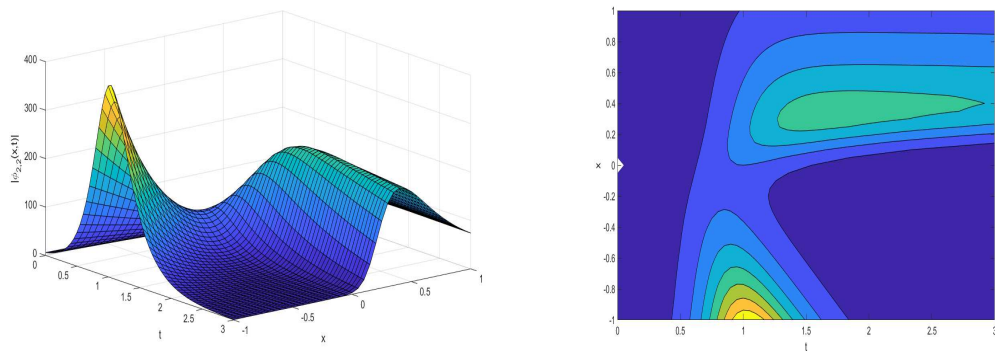


**Fig. 6.** 3-D and contour graphs of 27 for values of  $\tau = 150$ ,  $\alpha = 10$ ,  $P_0 = 10$ ,  $\kappa = 0,59$ ,  $\omega = 5$ ,  $\theta = 5$

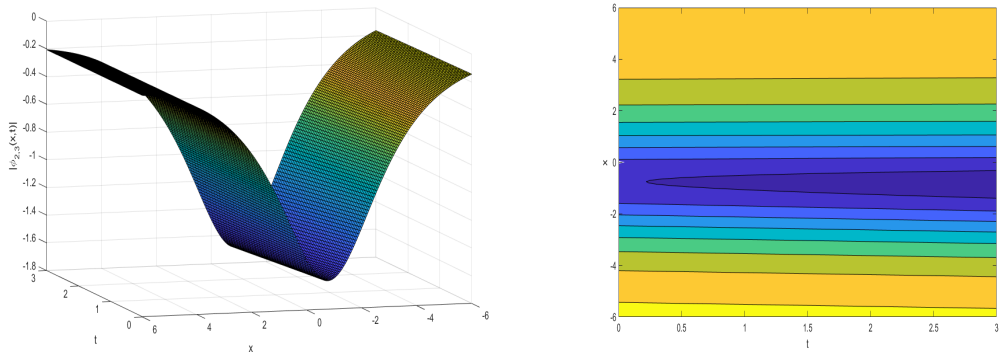


**Fig. 7.** 3-D and contour graphs of 28 for values of  $\tau = 0, 1$ ,  $\alpha = 1$ ,  $P_0 = 1$ ,  $\kappa = 0, 01$ ,  $\omega = 0, 01$ ,  $\theta = 1$

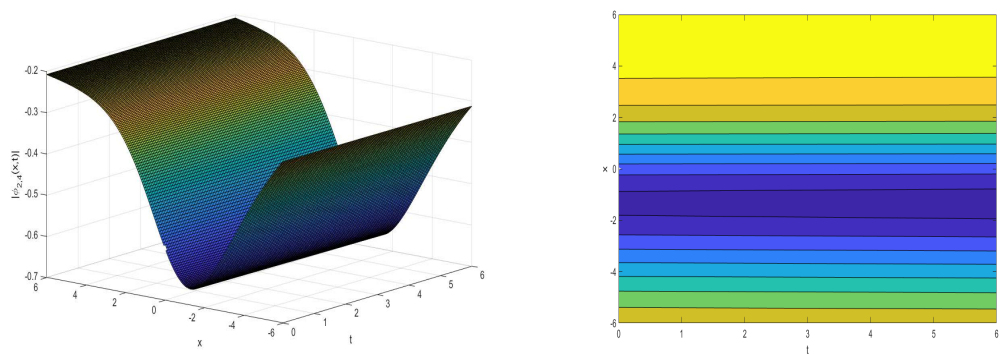


**Fig. 8.** 3-D and contour graphs of 29 for values of  $\tau = 0, 3$ ,  $\alpha = 1$ ,  $P_0 = 0, 01$ ,  $\kappa = 0, 0009$ ,  $\omega = 0, 001$ ,  $\theta = 1$

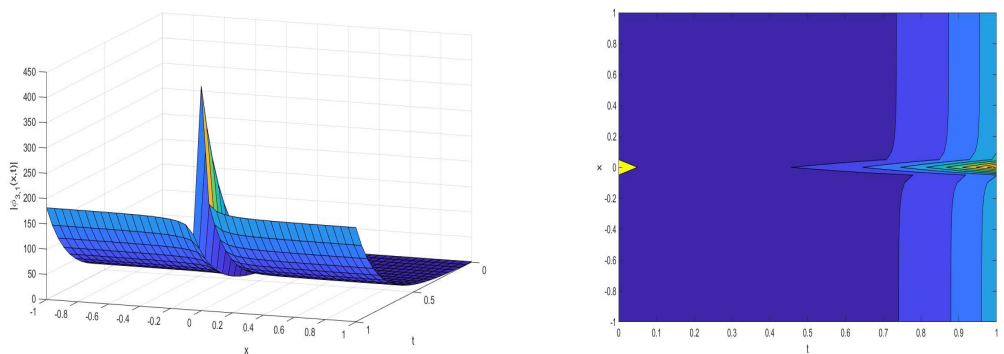


**Fig. 9.** 3-D and contour graphs of 30 for values of  $G = 50$ ,  $\tau = 2$ ,  $\alpha = 10$ ,  $P_0 = 0, 1$ ,  $\kappa = 0, 001$ ,  $\omega = 5$ ,  $\theta = 0, 1$

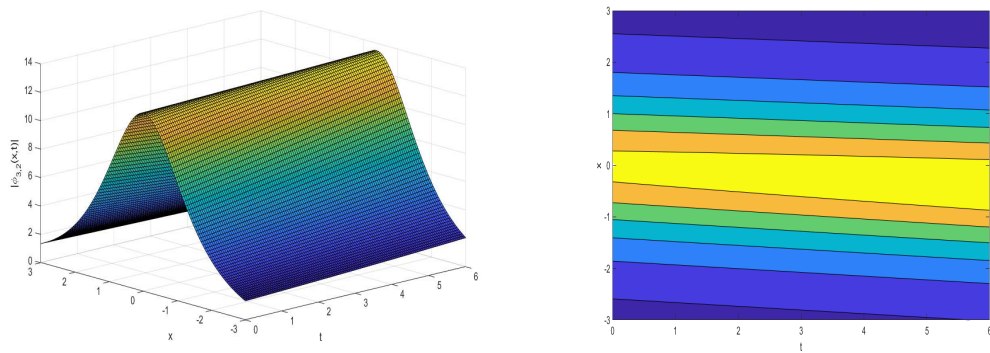


**Fig. 10.** 3-D and contour graphs of 31 for values of  $G = 1$ ,  $\tau = 100$ ,  $\alpha = 0, 1$ ,  $P_0 = 0, 1$ ,  $\kappa = 0, 01$ ,  $\omega = 0, 01$ ,  $\theta = 0, 01$

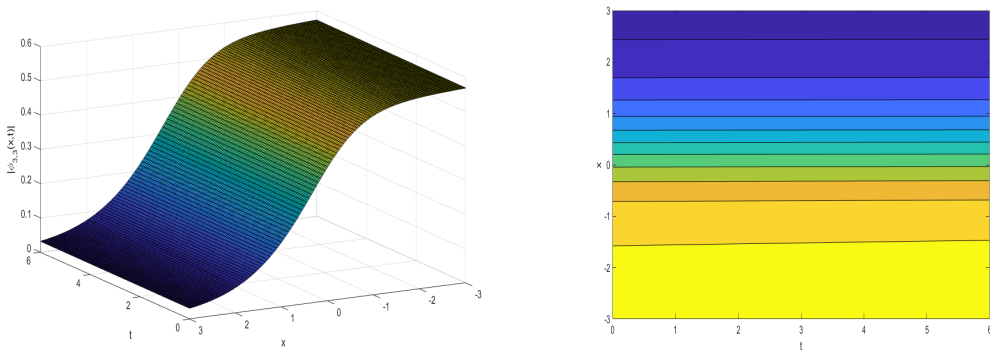


**Fig. 11.** 3-D and contour graphs of 32 for values of  $G = 0, 0001$ ,  $\tau = 0, 1$ ,  $\alpha = 2$ ,  $P_0 = 1$ ,  $\kappa = 0, 01$ ,  $\omega = 0, 001$ ,  $\theta = 0, 1$

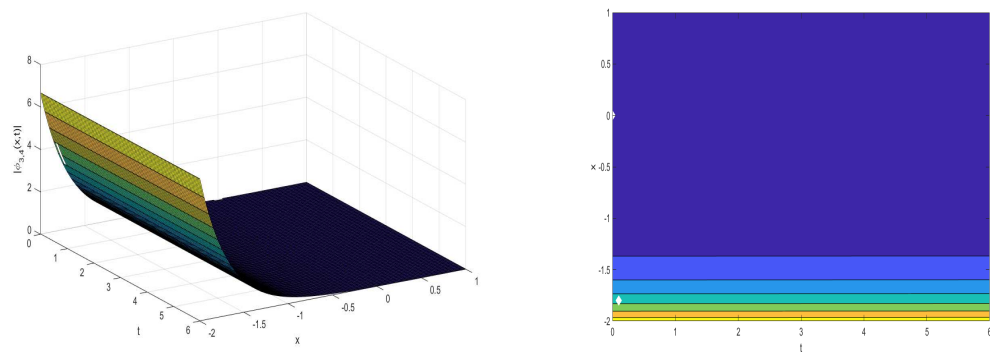


**Fig. 12.** 3-D and contour graphs of 33 for values of  $G = 1$ ,  $\tau = 1$ ,  $\alpha = 1$ ,  $P_0 = 0, 0001$ ,  $\kappa = 3$ ,  $\omega = 0, 001$ ,  $\theta = 0, 001$

#### 4. Physical Interpretation and Conclusion

The 3D and contour plots that are presented in the graphical representation section are used to visually represent the shape of the wave function and to showcase the physical

behavior of the solutions that are obtained. We discuss here the interpretation of these plots and their importance in understanding the characteristics of the solutions. Both the 3D plot and contour plot of the complex wave function are useful tools for visualizing the behavior of the wave function and can provide insights into the dynamics of the system. They can be used to identify the presence of solitons, nonlinear effects, and other interesting features of the wave function. The Figs. 10 display singular solitary wave solutions, and Figs. 2, 6 display combination of singular solitary wave solutions. Similarly, the Figs. 11, 12 display periodic wave solutions, and the Figs. 3, 4, 7, 8 display combination of periodic wave solutions. Furthermore, the figures 9 display bright solitary wave solution, and figures 1, 5 display combination of bright-dark solitary wave solution.

In this study, the traveling wave solutions of the 3d cubic focusing nonlinear Schrödinger equation with Woods–Saxon potential have been obtained successfully using the generalized projective Riccati equation method. In this study, we investigate bright and dark solitary wave, periodic wave, and other forms of exact solutions. The results we obtained that the generalized projective Riccati equation method is an excellent mathematical tool for finding exact solutions to nonlinear differential equations, such as the 3d cubic focusing nonlinear Schrödinger equation with Woods–Saxon potential. The determined solutions reveal important perception into the dynamics of wave propagation in nonlinear media with complex potentials and may find application in a number of physics and engineering disciplines. Our findings contribute to a deeper understanding of the behavior of the 3d cubic focusing nonlinear Schrödinger equation with Woods–Saxon potential and shed light on the nonlinear dynamics of wave propagation in physical systems with different potentials. The obtained solutions and their properties may find applications in various areas, such as in the design and optimization of nonlinear optical devices, quantum information processing, and quantum computing. The generalized projective Riccati equation method can be extended to other nonlinear equations in mathematical physics, and its applications can be further explored in future research.

## References

1. Onyenegecha C.P., Njoku I.J., Opara A.I., Echendu O.K., Omoko E.N., Eze F.C., Nwaneho F.U. Nonrelativistic Solutions of Schrodinger Equation and Thermodynamic Properties with the Proposed Modified Mobiüs Square Plus Eckart Potential. *Heliyon*, 2022, vol. 8, no. 2, article ID: e08952, 10 p. DOI: 10.1016/j.heliyon.2022.e08952
2. Wei Gao-Feng, Long Chao-Yun, Duan Xiao-Yong, Dong Shi-Hai. Arbitrary L-Wave Scattering State Solutions of the Schrodinger Equation for the Eckart Potential. *Physica Scripta*, 2008, vol. 77, no. 3, article ID: 035001, 5 p. DOI: 10.1088/0031-8949/77/03/035001
3. Morrison C.L., Shizgal B. Pseudospectral Solution of the Schrodinger Equation for the Rosen-Morse and Eckart Potentials. *Journal of Mathematical Chemistry*, 2019, vol. 57, no. 12, pp. 1035–1052. DOI: 10.1007/s10910-019-01007-2
4. Onate C.A., Akanbi T.A. Solutions of the Schrodinger Equation with Improved Rosen Morse Potential for Nitrogen Molecule and Sodium Dimer. *Results in Physics*, 2021, vol. 22, no. 6, article ID: 103961, 7 p. DOI: 10.1016/j.rinp.2021.103961
5. Desai A.M., Mesquita N., Fernandes V. A New Modified Morse Potential Energy Function for Diatomic Molecules. *Physica Scripta*, 2020, vol. 95, no. 8, article ID: 085401, 6 p. DOI: 10.1088/1402-4896/ab9bdc

6. Udo M.E., Okorie U.S., Ngwueke M.I., Ituen E.E., Ikot A.N. Rotation-Vibrational Energies for Some Diatomic Molecules with Improved Rosen-Morse Potential in D-Dimensions. *Journal of Molecular Modeling*, 2019, vol. 25, no. 6, pp. 1–7. DOI:10.1007/s00894-019-4040-5
7. Carbo-Dorca R., Nath D. Average Energy and Quantum Similarity of a Time Dependent Quantum System Subject to Poschl-Teller Potential. *Journal of Mathematical Chemistry*, 2022, vol. 60, no. 2, pp. 1–21. DOI: 10.1007/s10910-021-01318-3
8. Pereira L.C., Marangoni B.S., do Nascimento V.A. Dynamics and Stability of Matter-Wave Solitons in Cigar-Shaped Bose-Einstein Condensates Dragged by Poschl-Teller Potential. *International Journal of Quantum Chemistry*, 2021, vol. 121, no. 11, article ID: e26634, 9 p. DOI: 10.1002/qua.26634
9. Jaramillo B., Martinez-y-Romero R.P., Nunez-Yepez H.N., Salas-Brito A.L. On the One-Dimensional Coulomb Problem. *Physics Letters A*, 2009, vol. 374, no. 2, pp. 150–153. DOI: 10.1016/j.physleta.2009.10.073
10. Inyang E.P., William E.S., Obu J.A. Eigensolutions of the  $N$ -Dimensional Schrodinger Equation Interacting with Varshni–Hulthen Potential Model. *Revista Mexicana de Fisica*, 2021, vol. 67, no. 2, pp. 193–205. DOI: 10.31349/RevMexFis.67.193
11. Chen Lu, Lu Guozhen, Zhu Maochun. Sharp Trudinger-Moser Inequality and Ground State Solutions to Quasi-Linear Schrodinger Equations with Degenerate Potentials in  $\mathbb{R}^n$ . *Advanced Nonlinear Studies*, 2021, vol. 21, no. 4, pp. 733–749. DOI: 10.1515/ans-2021-2146
12. Lorca S., Montenegro M. Spike Solutions of a Nonlinear Schrodinger Equation with Degenerate Potential. *Journal of Mathematical Analysis and Applications*, 2004, vol. 295, no. 1, pp. 276–286. DOI: 10.1016/j.jmaa.2004.03.044
13. Wenbo Wang, Quanqing Li. Existence and Concentration of Positive Ground States for Schrodinger-Poisson Equations with Competing Potential Functions. *Electronic Journal of Differential Equations*, 2020, vol. 2020, no. 78, pp. 1–19.
14. Yan Zhenya, Wen Zichao, Konotop V.V. Solitons in a Nonlinear Schrodinger Equation with PT-Symmetric Potentials and Inhomogeneous Nonlinearity: Stability and Excitation of Nonlinear Mordinary Differential Equations. *Physical Review A*, 2015, vol. 92, no. 2, article ID: 023821, 8 p. DOI: 10.1103/PhysRevA.92.023821
15. Deng Yangbao, Deng Shuguang, Tan Chao, Xiong Cuixiu, Zhang Guangfu, Tian Ye. Study on Propagation Characteristics of Temporal Soliton in Scarff II PT-Symmetric Potential Based on Intensity Moments. *Optics and Laser Technology*, 2016, vol. 79, pp. 32–38. DOI: 10.1016/j.optlastec.2015.11.003
16. Znojil M. Exact Solution for Morse Oscillator in PT-Symmetric Quantum Mechanics. *Physics Letters A*, 1999, vol. 264, no. 2-3, pp. 108–111. DOI: 10.1016/S0375-9601(99)00805-1
17. Bo Wen-Bo, Wang Ru-Ru, Fang, Yin, Wang, Yue-Yue, Dai Chao-Qing. Prediction and Dynamical Evolution Of Multipole Soliton Families in Fractional Schrodinger Equation with the PT-Symmetric Potential and Saturable Nonlinearity. *Nonlinear Dynamics*, 2022, vol. 111, no. 2, pp. 1–12. DOI: 10.1007/s11071-022-07884-8
18. Midya B., Roychoudhury R. Nonlinear Localized Mordinary Differential Equations in PT-Symmetric Rosen-Morse Potential Wells. *Physical Review A*, 2013, vol. 87, no. 4, article ID: 045803, 5 p. DOI: 10.1103/PhysRevA.87.045803
19. Inc M., Iqbal M.S., Baber M.Z., Qasim M., Iqbal Z., Tarar M.A., Ali A.H. Exploring the Solitary Wave Solutions of Einstein’s Vacuum Field Equation in the Context of Ambitious Experiments and Space Missions. *Alexandria Engineering Journal*, 2023, vol. 82, pp. 186–194. DOI: 10.1016/j.aej.2023.09.071

20. Rehman, S.U., Nawaz R., Zia F., Fewster-Young N., Ali A.H. A Comparative Analysis of Noyes-Field Model for the Non-Linear Belousov-Zhabotinsky Reaction Using Two Reliable Techniques. *Alexandria Engineering Journal*, 2024, vol. 93, pp. 259–279. DOI: 10.1016/j.aej.2024.03.010
21. Yongyi Gu, Baixin Chen, Feng Ye, Najva A. Soliton Solutions of Nonlinear Schrodinger Equation with the Variable Coefficients under the Influence of Woods-Saxon Potential. *Results in Physics*, 2022, vol. 42, article ID: 105979. DOI: 10.1016/j.rinp.2022.105979
22. Zayed E.M.E., Alurrfi K.A.E. The Generalized Projective Riccati Equations Method for Solving Nonlinear Evolution Equations in Mathematical Physics. In *Abstract and Applied Analysis*, 2014, vol. 2014, article ID: 259190. DOI: 10.1155/2014/259190
23. Yao Shao-Wen, Akram G., Sadaf M., Zainab I., Rezazadeh H., Inc M. Bright, Dark, Periodic and Kink Solitary Wave Solutions of Evolutionary Zoomeron Equation. *Results in Physics*, 2022, vol. 43, article ID: 106117. DOI: 10.1016/j.rinp.2022.106117
24. Younis M., Sulaiman T.A., Bilal M., Rehman S.U., Younas U. Modulation Instability Analysis, Optical and Other Solutions to the Modified Nonlinear Schrodinger Equation. *Communications in Theoretical Physics*, 2020, vol. 72, no. 6, article ID: 065001, 12 p. DOI: 10.1088/1572-9494/ab7ec8

Received December 3, 2023

---

УДК 517.95

DOI: 10.14529/mmp240206

## ЭФФЕКТЫ СОЛИТАРНОЙ ВОЛНЫ ПОТЕНЦИАЛА ВУДСА – САКСОНА В УРАВНЕНИИ ШРЕДИНГЕРА С 3Д КУБИЧЕСКОЙ НЕЛИНЕЙНОСТЬЮ

*Мустафа Инк<sup>1</sup>, Мухаммад Саджид Икбал<sup>2,3</sup>, Али Хасан Али<sup>4,5,6</sup>,  
Зуха Манзур<sup>7</sup>, Фарра Ашраф<sup>7</sup>*

<sup>1</sup>Университет Фират, Элязыг, Турция

<sup>2</sup>Универсальный колледж Орикс с Ливерпульским университетом Джона Мурса, Доха, Катар

<sup>3</sup>Национальный университет наук и технологий, Исламабад, Пакистан

<sup>4</sup>Университет Басры, Басра, Ирак

<sup>5</sup>Университетский колледж Аль-Имам, Балад, Ирак

<sup>6</sup>Университет Аль-Айен, Ди-Кар, Ирак

<sup>7</sup>Университет Лахора, Пенджаб, Пакистан

В этой исследовательской статье мы применяем метод обобщенного проективного уравнения Риккати для построения решений бегущей волны 3D кубического фокусирующего нелинейного уравнения Шредингера с потенциалом Вудса – Саксона. Обобщенный проективный метод Риккати является мощным и эффективным математическим инструментом для получения точных решений нелинейных уравнений в частных производных и позволяет получить множество решений бегущей волны трехмерного кубического фокусирующего нелинейного уравнения Шредингера с потенциалом Вудса – Саксона. Эти решения содержат периодические волновые решения, светлые и темные солитонные решения. Исследование многих физических систем, таких как конденсаты Бозе – Эйнштейна и систем нелинейной оптики, приводят к нелинейному уравнению Шредингера. В статье дается подробное описание обобщенного проективного

метода Риккати и демонстрируется его полезность в решение нелинейного уравнения Шрёдингера с потенциалом Вудса – Саксона. В статье представлены различные графические представления полученных решений с помощью программного обеспечения MATLAB и проанализированы их характеристики. Представленные результаты дают новое представление о поведении трехмерного кубического фокусирующего нелинейного уравнения Шредингера с потенциалом Вудса – Саксона и имеют потенциальные приложения во многих областях физики, а также в нелинейной оптике и физике конденсированного состояния.

*Ключевые слова:* 3D кубическое фокусирующее нелинейное уравнение Шрёдингера; потенциал Вудса – Саксона; решение бегущей волны; метод обобщенного проективного уравнения Риккати (GPREM).

Мустафа Инк, Университет Фират (г. Элязыг, Турция), minc@firat.edu.tr.

Мухаммад Саджид Икбал, Универсальный колледж Орикс с Ливерпульским университетом Джона Мурса (г. Доха, Катар); Национальный университет наук и технологий (г. Исламабад, Пакистан), sajid606@gmail.com.

Али Хасан Али, Университет Басры (г. Басра, Ирак); Университетский колледж Аль-Имам (г. Балад, Ирак); Университет Аль-Айен (г. Ди-Кар, Ирак), ali.hasan@science.unideb.hu.

Зуха Манзур, Университет Лахора (г. Пенджаб, Пакистан), zuha.manzoor10@gmail.com.

Фарра Ашраф, Университет Лахора (г. Пенджаб, Пакистан), farrah.ashraf@math.uol.edu.pk.

*Поступила в редакцию 3 декабря 2023 г.*